Proton and Water Activity-Controlled Structure Formation in Zinc Carboxylate-Based Metal Organic Frameworks

Steffen Hausdorf, Jörg Wagler, Regina Mossig, and Florian O. R. L. Mertens*

TU Bergakademie Freiberg, Leipziger Strasse 29, D-09596 Freiberg, Germany

Received: November 20, 2007; Revised Manuscript Received: April 28, 2008

The contributions of terephthalic acid and Zn^{2+}-coordinated water in *N,N*-diethylformamide (DEF) to the overall proton activity in the synthesis of MOF-5 ($Zn_4O(BDC)_3$, BDC = 1,4-benzenedicarboxylate) were quantitatively determined by combined electrochemical and UV−vis spectroscopic measurements. Structural transformations of zinc carboxylate-based metal organic frameworks due to their exposure to environments with variable water concentrations and the chemical means necessary to revert these transitions have been investigated. It was found that the water-induced structural transition of MOF-5 to the hydroxide structure $Zn_3(OH)_2(BDC)_2 \cdot 2DEF$ (MOF-69c) can be reverted by a thermal treatment of the obtained compound and its subsequent exposure to anhydrous DEF. MOF-5 syntheses from simple carboxylates as well as a water-free synthesis based on nitrate decomposition are presented. The latter demonstrates that nitrate can serve as the sole source for the oxide ion in MOF-5.

1. Introduction

To date, a wide range of highly porous metal organic coordination polymers or frameworks have been discovered. However, the group of carboxylate-based MOFs, especially the MOF-5 analogues discovered by Yaghi and co-workers, still dominates this variety.[1–3] Among the many proposals on functionalization and potential application of these materials, the highest level of activity can be found in the areas of gas storage,[4–8] gas separation,[9,10] sensing,[11–13] and catalysis.[14–17] In particular, MOFs with carboxylic acid-based linkers are attractive because they allow, to a certain degree, implementing the concept of crystal engineering, i.e., to create predictable structures simply by varying the carboxylic acids.[1,18–21] In addition to controlling the MOF microstructure, a concept which is most successful if the organic linkers do not bear any further functional groups, there is also the desire to control the crystal growth properties in order to be able to deposit MOF material onto specific materials or in certain geometries,[22,23] be it for the development of sensing devices, tube reactors, or other applications. Crystallization experiments have already been part of the earliest experiments dealing with MOF-5. For example, the Yaghi group changed the synthesis of MOF-5 from the initial concept where the base NEt_3 for deprotonation of the carboxylic acid is being provided via gas-phase diffusion[24] to one where the base is being provided by a decomposition process of the solvent. This simplification significantly sped up the synthesis. Very recently, a microwave-assisted synthesis of MOF-5 material was reported in which MOF-5 formation was completed within minutes.[25]

To rationally develop processes and techniques ranging from growing smooth zinc carboxylate MOF layers to nanocrystalline materials, a thorough understanding of the reaction steps involved in the synthesis of these MOF types is required. In this respect, we previously reported a study of the composition changes occurring in the reaction solution and in the gas phase during the solvothermal synthesis of zinc carboxylate-based MOFs.[26] In accordance with the finding of other authors,[27–29] our results demonstrated and explained the important role of water in the classical MOF-5-type synthesis based on zinc nitrate and terephthalic acid in diethylformamide (DEF). As reported by Rosi et al., addition of water to the reaction solution suppresses formation of MOF-5, and formation of other structures such as MOF-69c and $Zn_3(NH_2Et_2)_2BDC_4$ is then favored.[31] From this observation and the fact that hydrolysis of the solvent DEF is needed to provide $HNEt_2$ as a base for deprotonation of the carboxylic acid as a prerequisite for the MOF formation, an ambivalent role of water arises. On one hand, it is essential for formation of the oxide-based zinc carboxylate MOF-5; on the other hand, it fosters its destruction. In our previous study we found that the standard synthesis in DEF combines several reaction pathways which are capable of either producing or removing water. These findings allowed us to postulate that, depending on the dominance of a specific pathway, either oxide-based or hydroxide-based structures are formed. Investigations of the gases released during the solvothermal synthesis indicate that, in a successful MOF-5 experiment, a switch from the water-producing to the water-removing pathways occurs. Release of molecular hydrogen during the reaction was interpreted as the Lewis-base-catalyzed ($HNEt_2$) decay of the thermodynamically unstable formic acid molecule that is formed by hydrolysis of the solvent DEF. These two reactions in conjunction, hydrolysis and formic acid decomposition, are the only means in the standard synthesis to provide base and remove formic acid without producing water.

Since the well-known porous structure, MOF-5, bears an oxide ion, which clearly would not be capable of surviving a very high proton activity, great care was taken in this work to measure the pH equivalent in the organic solvent DEF and also learn more about the role of the proton activity in the overall reaction scheme of zinc carboxylate-based MOFs. The investigations presented herein are a continuation of our previous work on the overall reaction scheme. Besides the proton activity, which is closely related to the role of water in the synthesis, we extended our investigation to other mechanistic aspects such as water and nitrate coordination on the zinc centers and the

* To whom correspondence should be addressed. E-mail:florian.mertens@chemie.tu-freiberg.de.

10.1021/jp7110633 CCC: $40.75
Published on Web 07/25/2008

stability of the product structures in DEF water mixtures, mapping out quantitatively the regions of practical stability. We also tested for the means necessary to reverse the observed transformations.

2. Experimental Procedures

General Experimental. Individual syntheses were carried out in an autoclave (Parr Instrument Co. 4740, 75 mL) with a glass liner. Screening experiments for evaluation of the stability regions of various MOFs and generation of a phase-diagram-like graph were performed in glass containers of 4 mL volume, which were put into self-built steel reaction vessels equipped with an overpressure release system. The vessels were filled with the reactants (DEF−water mixtures and 15 mg of the solid sample) at room temperature and brought to the temperature indicated in the diagram. In contrast to earlier assumptions, it can be stated that the pressure variations are of minor or no importance for MOF-5 creation. The ratio of the head-space volume to liquid-phase volume was typically 1:5. FTIR-ATR measurements were taken using a Nicolet 380 spectrometer with a MCT detector equipped with an ATR (Golden Gate Specac). The Raman spectra were recorded on a Bruker RFS 100/S, (Neodym YAG Laser) instrument. Solid precipitates were analyzed by X-ray powder diffraction (Siemens D5000 using the Cu Kα line), whereas single-crystal X-ray diffraction data were collected on a Bruker AXS X8 diffractometer with Apex II area detector using Mo Kα radiation. The recorded data were evaluated using the SHELXTL program package. The crystallographic data for the structure of H_2NEt_2(HBDC) have been deposited with the Cambridge Crystallographic Data Centre as supplementary publication no. CCDC-667675. Basic structural data of H_2NEt_2(HBDC) are as follows: monoclinic, $P2_1/c$, a = 14,0720(5) Å, b = 8.0664(3) Å, c = 10,8823(4) Å, $\alpha = 90°$, $\beta = 92.837(2)°$, $\gamma = 90°$). Proton activities or pH analogues in organic solvents were measured by a self-built electrochemical cell using two H_2/Pd electrodes (palladium coated Pt electrodes) and salt bridges containing LiCl/DEF solutions. Palladium instead of platinum was chosen as electrode material because of its lower tendency to promote redox reactions between the organic components and nitrate, which could have led to undesired electrical potential changes. The electrodes were prepared by galvanization of Pt electrodes with a 2 M HCl, 0.07 M H_2PdCl_6 solution (I/A = 20 mA/cm^2, t = 20 min).

Synthesis. A standard MOF-5 and MOF-69c synthesis is defined by the following protocol. The solvent *N,N*-diethylformamide (DEF, ABCR 99%) was dried over CaH_2 at 100 °C for about 1 h until no more hydrogen evolution was observed. In all reaction solutions the concentration of $Zn(NO_3)_2$ was 0.3 M and that of H_2BDC (Aldrich, 98%) was 0.1 M. The standard MOF-5 synthesis was carried out with $Zn(NO_3)_2 \cdot 4H_2O$ (Merck, 98.5%), but for the MOF-69c a zinc to water ratio of 1:8 was used. The solutions were prepared in an argon-filled glovebox and only briefly exposed to air during the filling of the autoclave. The autoclaves were heated and kept at 105 °C. After 15 h small transparent crystals began to appear. After completion of the experiment after 20−24 h the crystals were checked by XRPD and the diffractogram indicated the presence of MOF-5 exclusively. For some experiments a water-free solution of zinc nitrate in DEF was prepared by dissolving anhydrous $ZnCl_2$ (Riedel-de Haën) and $AgNO_3$ (KMF Laborchemie Handels-GmbH) in dried DEF and the filtration of the resulting AgCl precipitate. To avoid any water contamination, preparation of the reaction solutions and filling of the autoclaves were also carried out under an argon atmosphere.

3. Results and Discussion

Proton Activity Measurements. As shown in our previous study,[26] control of the water content is fundamental for formation of oxide-based zinc carboxylates, i.e., MOF-5 analogues. The formal reaction equation of this process, $4Zn(NO_3)_2 \cdot 4H_2O + 3H_2BDC \rightarrow Zn_4O(BDC)_3 + 15H_2O + 8HNO_3$, demonstrates that there must be an efficient means to eliminate the strong acid HNO_3. As the major pathways affecting water and proton activity we identified steps that are water reducing and base producing

$$HC(O)NEt_2 + H_2O \rightarrow HCOOH + HNEt_2 \rightleftharpoons HCOO^- + H_2NEt_2^+ \quad (1)$$

acid (formic acid) removing

$$HCOO^- + H_2NEt_2^+ \rightarrow CO_2 + H_2 + HNEt_2 \quad (2)$$

and water producing

$$HCOOH + HNO_3 \rightarrow CO_2 + HNO_2 + H_2O \quad (3a)$$

$$2HCOOH + HNO_3 \rightarrow 2CO_2 + 0.5N_2O + 2H_2O \quad (3b)$$

and we additionally found indications for the reaction

$$HNEt_2 + HNO_2 \rightarrow Et_2NNO + H_2O \quad (4)$$

At the same time it is not clear to which extent the individual components contribute to the overall proton activity and how the water and proton activities are related to one another. Furthermore, it is well known that coordination of water to metal cations such as zinc increases its acidity, another process which influences the proton activity.

$$H_2O[Zn^{2+}] + HNEt_2 \rightarrow OH^-[Zn^{2+}] + (H_2NEt_2)^+ \quad (5a)$$

$$[Zn(H_2O)_n]^{2+} \rightleftharpoons [Zn(OH)(H_2O)_{n-1}]^+ + H^+ \quad (5b)$$

We intended to quantitatively determine the proton activity and dissociation constants in the reaction solution by cell voltage measurements between one half-cell containing a reference solution with a known proton concentration and electrode potential and the other half-cell containing the reaction solution with the proton content to be determined. However, the simple electrochemical determination of such a pH analogue in an organic solvent is a nontrivial task since the water-based pH standard cannot simply be used as the reference system to measure proton base dissociation equilibria. Two electrochemical half-cells using electrolytes based on two different solvents brought into direct contact or in contact mediated via a salt bridge or generally an ion conducting contact generate an unknown potential difference $U_{Contact}$ caused by the diffusion potential U_D and the liquid junction potential U_{LJ}.

$$U_{Contact} = U_{LJ} + U_D \quad (6)$$

Consequently, the unknown proton activity in one half-cell cannot be deduced from a known activity in the other half-cell without knowing U_{LJ} and U_D. Although relative measurements of the acid dissociation would be possible, we set out to determine K_a of the terephthalic acid in DEF as well as the influence of the zinc-coordinated water to the overall proton activity. In order to do so we applied special procedures to determine the diffusion potential experimentally and develop a means to measure the proton activity in DEF or better the activity of the H^+−solvent adduct ($H(DEF)^+$) directly without using a water-based electrolyte. This in turn required development of a DEF-based reference half-cell instead of a water-

based one with known proton activity and introduction of a new DEF-based electrochemical standard called ^{DEF}pH, i.e., the analogue to the water-based pH standard. With these prerequisites fulfilled, the proton activity measurements can simply be carried out using DEF-based electrolytes only, and thus, formation of a liquid junction potential is avoided. Elimination of the liquid junction potential is important since it can be comparably large. For instance, a value of 172 mV has been measured for U_{LJ} across the interface H_2O/DMF using tetraphenylarsonium and tetraphenylborate electrodes,[31] which relates to a pH difference of ca. 2.9. In order to develop the ^{DEF}pH standard, we first had to find a new reference solution of a known proton activity or better of known H^+−solvent adduct ($HDEF^+$) activity that conceptually replaces the H_3O^+ activity in water-based systems. For simplicity reasons the $HDEF^+$ concentration of this reference system needs to be kept low enough that one can equate activity and concentration. The protocol according to which the DEF-based, chemically stable electrochemical reference was developed is as follows.

(A) Generation of a DEF solution with known $HDEF^+$ content. (1) Identifiying a suitable Brønsted acid (indicator) whose degree of dissociation in DEF can be determined spectroscopically (UV−vis). (2) Determining the UV−vis molar absorptivity of the protonated and deprotonated forms to measure their contents spectroscopically. (3) Determining of the pK_a value via $K_a = [H^+][Ind^-]/[HInd] = [Ind^-]^2/[Hind]$. (4) Preparing an indicator−DEF solution with a known $HDEF^+$ content.

(B) Preparation of a stable, i.e. buffered, electrochemical reference half-cell with a known $HDEF^+$ concentration against which unknown $HDEF^+$ concentration (activites) can be determined by cell voltage measurements. (1) Calculating the cell potential of the Pd|H_2, indicator−DEF half-cell via the Nernst equation by defining the standard potential of a solution with the activity $a(HDEF^+) = 1$ as $E° = 0$ V. (2) Preparation of a new buffered reference solution. (3) Determination of the half-cell potential of the buffered reference by measuring the potential difference to the indicator−DEF solution.

By identifying a suitable indicator compound that changes its light absorption properties in the UV−vis range according to the degree of deprotonation one can derive the degree of dissociation from UV−vis spectroscopy. As potential candidates we tested phenolphthaleine, thymolsulfonphthaleine, *p*-xylenolsulfonphthaleine, neutral red w, phenolsulfonphthalein, *p*-nitrophenol, and *o*-nitrophenol and found that only *o*- and *p*-nitrophenol reveal suitable absorption bands of the protonated and deprotonated forms in DEF in the appropriate spectral range (as can be seen in Figure 1 where the absorbance or logarithmic intensity loss $A = \log I_0/I$ is plotted against the wavelength). It is worth mentioning that neutral red and phenolsulfonphthaleine, which are very weak acids in water, act as strong acids in DEF. Because of the better separation of the absorption bands for the dissociated and nondissociated species, we used *o*-nitrophenol for the subsequent experiments. *o*-Nitrophenol has its absorption maximum at 340.3 nm, whereas for the deprotonated form, the phenolate anion, the absorption maximum is shifted to 441.7 nm. As the spectra demonstrate, both absorption signals are sufficiently separated so that they can simply be evaluated by either integration or determination of the peak height which can also serve as an approximate measure for the concentration of the absorbing species.

To investigate the dissociation equilibrium of the terephthalic acid in DEF, an electrochemical cell was used consisting of two hydrogen palladium electrodes. A stable reference system

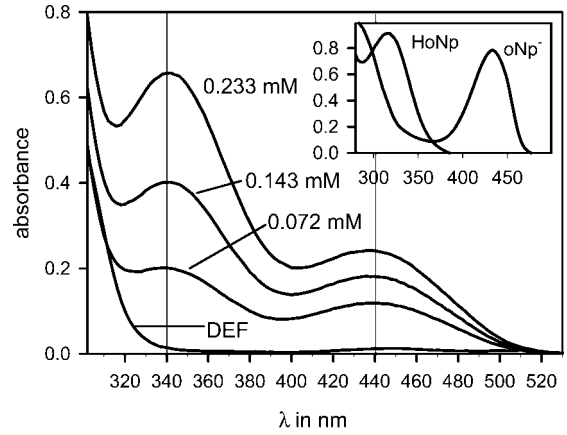

Figure 1. UV−vis spectra of pure DEF and *o*-nitrophenol−DEF solutions at various concentrations. Undissociated nitrophenol displays its absorption maximum at 340.3 nm and the nitrophenolate ion at 441.7 nm. The molar absorptivity of nitrophenol and the nitrophenolate ion was determined as 3.08 L mmol^{-1} cm^{-1} and 5.60 L mmol^{-1} cm^{-1}, respectively. K_a (*o*-nitrophenol) was determined by linear regression of $[oNp^-]^2$ as a function of [HoNp] resulting in $K_a = (9.2 \pm 0.2) \times 10^{-6}$ mol/L, p$K_a = 5.04 \pm 0.01$. The ^{DEF}pH of *o*-nitrophenol solutions were determined photometrical via pH = pK_a − log[HoNp] + log[oNp^-]. The insert shows the spectra of the fully protonated and deprotonated forms produced by adding traces of H_2SO_4 and Et_2NH.

(secondary reference) was generated by immersing one hydrogen palladium electrode in a 0.1 M buffer solution of LiCl in DEF saturated with (H_2NEt_2)HBDC and $(H_2NEt_2)_2$BDC at 25 °C. Therefore, the overall cell reads as Pd|H_2, (H_2NEt_2)HBDC(s), $(H_2NEt_2)_2$BDC(s), DEF||LiCl, DEF 1 M||Pd|H_2. The half-cell potential of this buffered reference electrode was determined against an *o*-nitrophenol solution (primary reference) the ^{DEF}pH value of which was UV−vis-spectroscopically determined. We obtained for the $HDEF^+$ concentration a value of $c(HDEF^+) = 10^{-4.61}$ mol/L which corresponds to a ^{DEF}pH value of 4.61. By approximating the $HDEF^+$ activity in the Nernst equation $E = E° + (RT/F)\ln[a(HDEF^+)/\phi(H_2)]$ by the concentration value and setting the H_2 fugacity to $\phi(H_2) = f\,p(H_2)/p° = 1$ as well as setting $E° = 0$ (this is the step that defines the $HDEF^+$ activity of the new standard ^{DEF}pH as equal to 1) yields for the theoretical electrode potential E_{th} at the given concentration $c(HDEF^+) = 10^{-4.61}$ mol/L

$$E_{th}(o\text{-nitrophenol}) = -272.0\ \text{mV} \qquad (7)$$

To switch from the *o*-nitrophenol solution-based primary reference to the solution buffered with (H_2NEt_2)HBDC and $(H_2NEt_2)_2$BDC)) as secondary reference, we measured the cell potential difference between these two half-cells, which resulted in

$$U_{eq}(\text{buffer against } o\text{-nitrophenol}) = -127.96\ \text{mV} \quad (8a)$$

Since both the reference half-cell and the salt bridge are now DEF based, the liquid junction potential is eliminated. To determine the influence of the diffusion potential we applied a semiempirical method proposed by Bjerrum et al.,[32] which assumes an inversely proportional dependence between the electrolyte concentration in the salt bridge and the diffusion potential difference. We therefore measured the cell voltage at various LiCl concentrations *c* in the salt bridge and extrapolated the data according to $1/c \rightarrow 0$. The linear dependence of the cell voltage from 1/*c* shown in Figure 2 demonstrates that this relationship is excellently fulfilled. The extrapolation to very high (infinitely high) concentrations determines the value of the

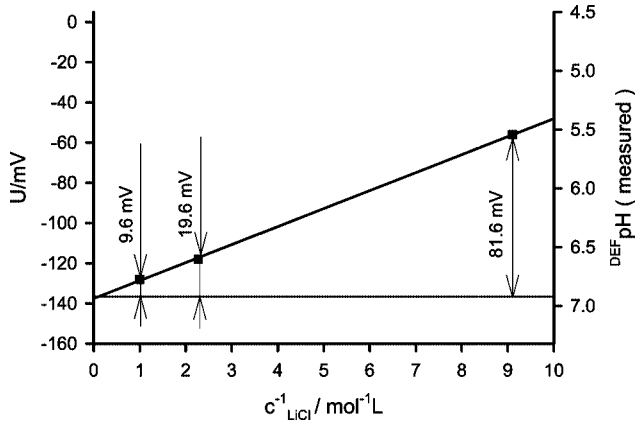

Figure 2. Example of the cell voltage dependence from the salt bridge electrolyte concentration. The extrapolation to high concentrations can be used to determine the diffusion potential via $U_D = U_{eq}(c) - U_{eq}(1/c \rightarrow 0)$ according to Bjerrum.[32] For the extrapolation, solutions of LiCl in DEF at three different concentrations were used. The correlation between U_{eq} and $1/c$ in the indicated range is almost perfectly linear. The diffusion potential for a 1 M LiCl−DEF solution was determined to be $U_D = 9.6$ mV.

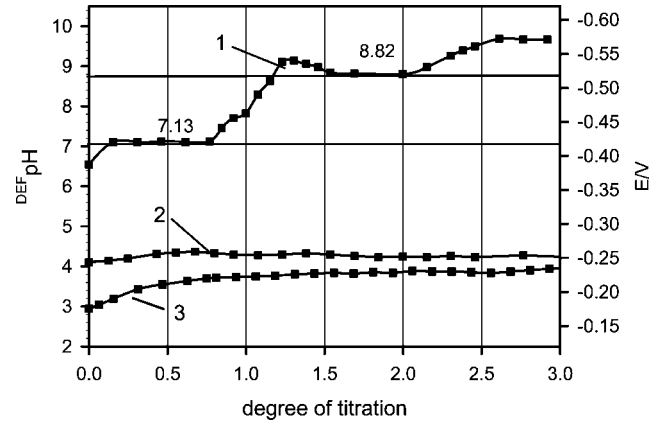

Figure 3. Titration experiments with diethylamine of different reactant mixtures derived from the standard MOF-5- synthesis solution: (1) 0.1 M H_2BDC/DEF, during titration precipitation of solid $(H_2NEt_2)HBDC$ and $(H_2NEt_2)_2BDC$ was observed; (2) 0.3 M $Zn(NO_3)_2 \cdot 4H_2O$/DEF; (3) 0.1 M H_2BDC/0.3 M $Zn(NO_3)_2 \cdot 4H_2O$/DEF (MOF-5 synthesis solution), titration was accompanied by precipitation of solid $Zn_5(OH)_4(BDC)_3$. The amount of the titrant diethylamine used is expressed for all three cases as the degree of titration of case 1).

cell potential without a diffusion voltage contribution. Thus, the difference between the voltage measured at a certain concentration and the extrapolated value yields the diffusion potential contribution.

According to Figure 2, the diffusion voltage for a 1 mol/L LiCl concentration in the salt bridge is given as 9.6 mV or 0.16 ^{DEF}pH. The previously determined value for U_{eq} for the buffered secondary reference against the primary was corrected by this value to

$$U_{eq,corr} = -137.56 \text{ mV} \quad (8b)$$

From this value we obtained the electrode potential E_m for the secondary reference by

$$U_{eq,corr} = E_m - E_{th} \Rightarrow U_{eq,corr} + E_{th} = E_m = -409.46 \text{ mV} \quad (9)$$

which corresponds to ^{DEF}pH(buffer) = 6.94.

We now have established a stable reference electrode/electrolyte system, or better half-cell, with a known H^+−solvent adduct activity against which all further measurements of ^{DEF}pH values can be taken. To agree with the measurements establishing this secondary reference, all further electrochemical experiments were also performed at 25 °C using a LiCl/DEF salt bridge.

The diffusion voltage was eliminated in all following measurements according to the Bjerrum method just described. In titration experiments the diffusion voltage was eliminated by taking the average of a measurement at the start and end of the titration experiment. In all cases the diffusion voltage was not larger than 10 mV or 0.17 ^{DEF}pH, respectively. Figure 3 displays the titration measurements of all individual components of the standard MOF-5 synthesis in DEF using diethylamine as the titrant. Diethylamine was chosen, on one hand, to avoid water production that would have resulted from hydroxide-containing bases, and on the other hand, it is the base that is produced during the MOF-5 synthesis by solvent hydrolysis. The upper curve in Figure 3 represents the titration of a 0.1 M solution of H_2BDC in DEF. The graph clearly displays the two deprotonation steps of the terephthalic acid. The titration was accompanied by precipitation of the organic salts $(H_2NEt_2)HBDC$ (first plateau) and $(H_2NEt_2)_2BDC$ (second plateau). Equilibration of the precipitates with the solution occurred with a significant delay, so that depending on speed of the titration several nonequilibrium effects can be observed, such as the overshooting right before reaching the second plateau and the shift of the second equivalence point from the theoretical value of 2 to ca. 2.5 instead of 2. The titration curve was recorded allowing 20 min equilibration time per each additional base dose.

From these measurements the degree of dissociation can be estimated if the presence of the buffer effect caused by the precipitates is taken into account. For the analysis of the first deprotonation step we separately determined the solubility product of the precipitate $[H_2NEt_2^+][HBDC^-]$ in DEF by the following steps. First, we prepared a clear 0.04 M solution of diethylammonium hydrogen terephthalate at 90 °C. Cooling this solution to 25 °C results in precipitation of $[H_2NEt_2^+][HBDC^-]$. Afterward, we carried out multiple temperature cycles between 90 and 25 °C with subsequent additions of DEF until no precipitation could be observed. The corresponding final concentration was 14.1 mmol/L, which yields for the solubility product $K_{sp} = [H_2NEt_2^+][HBDC^-] \approx [HBDC^-]^2 = 10^{-3.7}$ mol^2 L^{-2}. From the value of the first plateau at ^{DEF}pH = 7.13 and with the assumptions pK_a $(H_2NEt_2^+) \gg pK_a$ (H_2BDC), $[H_2NEt_2^+] = [HBDC^-]$, $[H_2BDC] = 0.5c_0$ one can derive

$$K_{a,1} \approx \frac{[HDEF]\sqrt{K_{sp}}}{0.5c_0}$$

$$pK_{a,1} = {}^{DEF}\text{pH} + 0.5pK_{sp} - \log(2) + \log c_0 = 7.68 \quad (10)$$

For the second deprotonation step one can similarly calculate from $pK_{sp} = 4.0$ and a plateau value of ^{DEF}pH = 8.82 a value of 9.2 for $pK_{a,2}$. However, the assumption of $pK_a(H_2NEt_2^+) \gg pK_a(HBDC^-)$ might not be valid anymore. These values show that terephthalic acid acts as a weak acid with a degree of dissociation of $\alpha_{max} = 0.05\%$ in DEF. This strongly contrasts the high degree of protolysis of other acids that are weak in water-based systems such as neutral red and phenol red. The second curve from the top in Figure 3 is a titration measurement of a 0.3 M solution of $Zn(NO_3)_2 \cdot 4H_2O$ in DEF as it is used in the standard MOF-5 synthesis. Protolysis of the Zn^{2+} hydrate (reaction 5b) leads to a ^{DEF}pH value of 4.23, which clearly indicates that the acidity of the solution is mainly determined

by the transition-metal hydrate and not by the carboxylic acid. The buffer capacity of the $Zn(NO_3)_2 \cdot 4H_2O$ solution is large enough that the amount of base added shows no effect and results in a perfectly flat plateau (for the two lower titration curves, the amount of base added is also given for comparison purposes by the degree of titration that belongs to the topmost curve). The bottom curve displays the result of a titration experiment which is a combination of the previous two, being the titration of a solution $Zn(NO_3)_2 \cdot 4H_2O$ and H_2BDC in DEF with the concentrations 0.3 and 0.1 M, respectively. As expected, the weak acid H_2BDC is not titrated in the presence of the comparably strong acid $[Zn(H_2O)_n]^{2+}$. A buffer effect occurs due to precipitation of $Zn_5(OH)_4BDC_3$, which was identified by XRPD. The solution is much more acidic than the pure $Zn(NO_3)_2 \cdot 4H_2O$−DEF solution and displays a significantly lower plateau value with $^{DEF}pH = 2.9$. The increase of the $HDEF^+$ concentration by $10^{-2.92}$ mol/L is best explained by coordination of $HBDC^-$ to the Zn^{2+} centers according to

$$H_2BDC + Zn^{2+} + DEF \rightleftharpoons [ZnHBDC]^+ + HDEF^+ \quad (11)$$

Given the initial concentration this corresponds to a degree of coordination of 1.2%. This indirect demonstration of the carboxylate coordination already in solution may also serve as a first indicator how the MOF-5 crystallization occurs. It demonstrates that the apparent contradiction between the high acidity of the solution and the stability of the salts of a weak acid, such as ZnBDC, MOF-69c, and MOF-5, is resolved by the presence of a sufficiently strong interaction of the carboxylate with the zinc center. At the same time the high acidity will help to keep enough terephthalate or hydrogen terephthalate in solution to prevent rapid precipitation of simple zinc terephthalates. It is also important to note that ^{DEF}pH measurements of the reaction solutions directly prior to and after a MOF-5 synthesis show that the ^{DEF}pH value changes less than 0.5 over the course of the experiment.

Structure of $H_2NEt_2(HBDC)$. The compound that precipitated during the titration experiment with terephthalic acid in DEF with diethylamine is of interest since among the many terephthalate structures that are related to the MOF-5 standard synthesis it must mark one limit structure for very basic reaction conditions with respect to this class of MOF synthesis procedures. We therefore determined its structure by single-crystal XRD measurement. In experiments using the MOF-5 standard recipe with 10 water molecules per Zn^{2+} added we also observed formation of $H_2NEt_2(HBDC)$ as identified by the same XRPD pattern. Since it can be assumed that in cases of high water content in the reaction solution there is much $HNEt_2$ base produced by the solvent hydrolysis both situations, high water content synthesis and formation during the titration experiment, are equivalent. From the water-based formation of $H_2NEt_2(HBDC)$ we obtained single crystals large enough for the single-crystal XRD measurement. Elements of the structure are shown in Figure 4. The nonporous structure consists of chains of hydrogen terephthalate units tied together via hydrogen bonds between one oxygen atom of the deprotonated carboxylate groups and the hydrogen atom of the remaining carboxylate groups of the neighboring terephthalic units, thus forming poly(hydrogen-terephthalate) chains. To achieve charge balance the structure bears the corresponding number of diethylammonium ions. The monoclinic unit cell ($P2_1/c$, $Z = 4$) contains four $H_2NEt_2^+(HBDC)$. The asymmetric unit consists of a diethylammonium cation, 2/2 terephthalate moieties, which are located on crystallographically imposed centers of inversion, and the formal hydrogenterephthalate−proton H1, which has

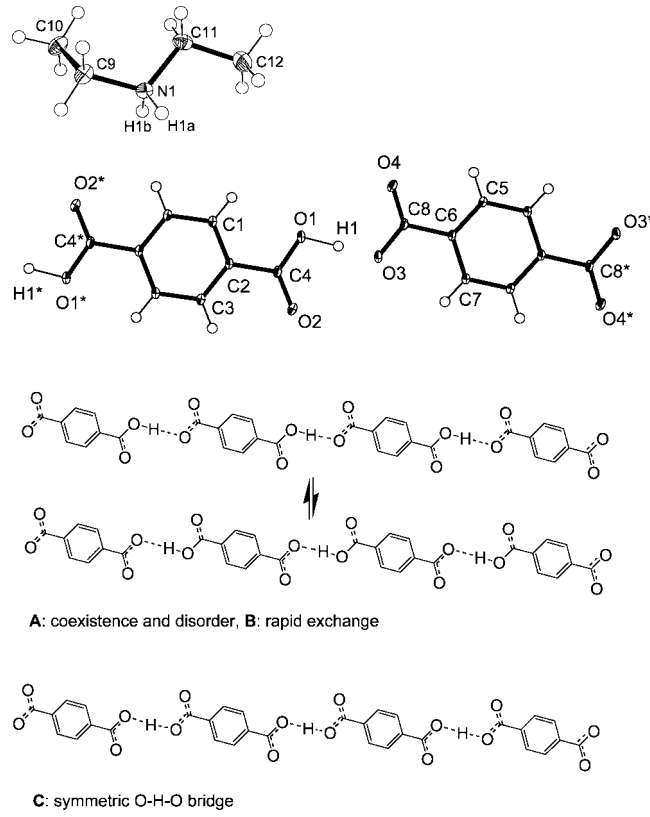

Figure 4. (Top and Middle) ORTEP plot (showing 50% probability ellipsoids) of the cation and a section of the polymeric anion within the structure of $H_2NEt_2^+(HBDC)^-$, respectively. Selected atoms of the asymmetric unit are labeled; the labels of selected symmetry-equivalent atoms are asterisked. (Bottom) Models A, B, and C, which would account for the polymeric anion found in the structure of $H_2NEt_2^+(HBDC)^-$.

been located almost midway between the oxygen atoms O1 and O3 (O1−H1 1.176(10) Å, O3−H1 1.271(10) Å). According to the crystallographically imposed symmetry of the polymeric anion, two protons would belong to the terephthalate bearing O1 and its symmetry-equivalent O1*, whereas the other terephthalate moiety, the one bearing O3 and O3*, would have to be referred to as a dianion. The similar O−H separations to O1 and O3, however, account for an almost equally shared O−H−O bridging contact. Although the hydrogen atom H1 could be well located from residual electron density maps and was isotropically refined without any restraints, the structure is constrained by the $P2_1/c$ space group symmetry operations and one can not fully exclude one of the bonding patterns A, B, and C (Figure 4) since in A and B the hydrogen atom H1 would be the only atom to break the space group symmetry, and the contribution of one H atom in such a position to the overall diffraction pattern cannot be expected to be the entire support for a structure model of lower symmetry. Therefore, the symmetrically constrained O−H−O bridge within this structure has to be discussed carefully. The fact that the isotropic thermal displacement parameter ($\times 10^3$ Å^2) of hydrogen atom H1 refined to 58(3), whereas the values for the N-bonded hydrogen atoms H1a and H1b are 30(2) and 26(2), respectively, hints to either a disorder of H1 by symmetry or a rapid exchange between O1−H1 and O3−H1 (models A and B, respectively). Furthermore, effects of the cation on a favorable position of H1 cannot be derived since the N−H protons form hydrogen bridges to the terminal oxygen atoms O2 and O4 of both terephthalate moieties (with N−H···O separations being N1−H1b−O1 0.93(1), 2.14(1) Å and N1−H1a−O4 1.00(1), 1.81(1) Å).

It is worth mentioning that in the N-unsubstituted ammonium hydrogenterephthalate $NH_4^+(HBDC)^-$ ($C2/c$, $Z = 4$) a similar polymeric anion is found and the O−H groups have been refined to provide a model which is related to model A in Figure 4, the O−H···O vs O···H−O disorder of which is also caused by symmetry constraints of the space group.[33] Selected crystallographic of parameters can be found in the Experimental Procedures.

Since the structural investigations also confirm that the base $HNEt_2$ is not strong enough to doubly deprotonate the terephthalic acid in DEF, even without the presence of water as seen in the titration experiment, we conclude that the second deprotonation step in formation of MOF-5 occurs after inclusion of the terephthalic acid unit into the MOF lattice, thus ensuring an ordered and slowed down crystal growth process.

Nitrate and Water Coordination on Zinc Centers. On one hand, as seen in the proton activity measurements, water coordination to the zinc center is responsible for the high acidity of the solution that keeps the terephtalic acid in the presence of zinc ions in solution. On the other hand, we performed an experiment resulting also in MOF-5 without the presence of water at all. Starting from a water-free solution of DEF with zinc nitrate and terephthalic acid prepared according to the recipe described in the Experimental Procedures, we found that keeping the solution at temperatures of 130−140 °C for 5−6 h leads eventually to formation of MOF-5. After 30 min one can first observe precipitation of needle-shaped crystals of ZnBDC·DEF, which then are slowly transformed into small cubic-shaped crystals of MOF-5. Both compounds have been identified by XRPD. The ZnBDC·DEF XRPD diffractogram was simulated from the structural data to be found in ref 34. In continuation to our previous study,[26] we also looked at the composition of the gaseous products released during this synthesis, which contained less CO_2 but instead a significant amount of N_2 compared to the standard synthesis based on zinc nitrate containing water of crystallization. This result also indicates a strongly altered reaction pathway. One of the reaction products is water, and at the end of the process a zinc to water ratio of 1:1 is reached as determined by Karl Fischer titration. In order to learn in this respect more about the water and the nitrate coordination properties we conducted IR-ATR and Raman spectroscopy measurements of a zinc nitrate−DEF solution as a function of the water content. The results are shown in Figure 5. Displayed is a region of the IR and the Raman spectrum close to the symmetric stretch frequency ($\nu_s = 1050$ cm^{-1}) of free nitrate in which the solvent DEF is free of vibrational modes. A spectrum of pure DEF is also shown in the figure for reference purposes. The Raman spectra taken do not show any signs of the presence of free nitrate for all water contents, although water could have been expected to be the more strongly bonding ligand. However, the IR spectra display two frequencies at 1040 and 1027 cm^{-1}. The signal at 1040 cm^{-1} is strongest at the water content of $6H_2O$ per zinc ion and almost vanishes at water-free conditions. Since this wavenumber is still close to the one of free nitrate, we also interpret this frequency essentially as the symmetric stretch vibration shifted from 1050 to 1040 cm^{-1} by coordination to the zinc atom. Although the symmetric stretch vibration of free nitrate is symmetry forbidden in IR measurements, it can be seen because of the symmetry breaking caused by coordination to the zinc center. In respect to the wavenumber shift from 1040 to 1027 cm^{-1} with decreasing water content, similar results can be found in the literature. Although Sze and Irish[35] report for highly concentrated solutions in water a wavenumber of 1040 cm^{-1} belonging to a zinc mononitrato hydrate complex, we assume that this value belongs to a zinc dinitrato hydrate complex in our case because we did not find uncoordinated nitrate. They also observed a shift from 1040 to 1025 cm^{-1} for nitrate coordination if water−acetonitrile solutions are used and the water content is sufficiently lowered.[36] The authors attribute the value 1025 cm^{-1} to the $[Zn(NO_3)(CH_3CN)_2]^+$ complex. A similar phenomenon based on DEF coordination may explain the 1027 cm^{-1} frequency appearing in our low water content measurements. In conclusion, even at high water contents we did not find in these experiments that nitrate is largely replaced by water or solvent molecules. Coordination and consequently distortion of the nitrate molecule must be seen as the origin of nitrate decomposition similarly to decomposition of transition-metal nitrates in solids.

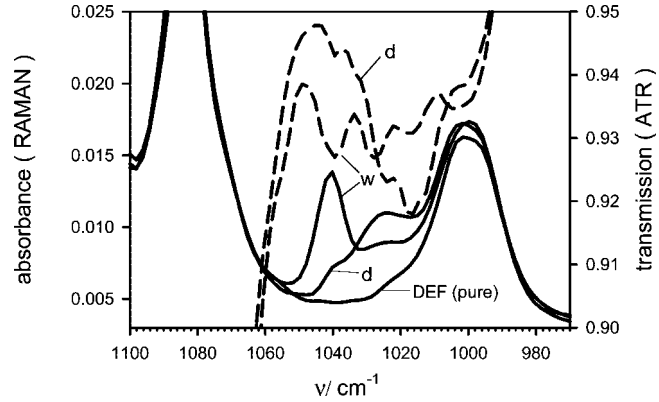

Figure 5. Raman (full line) and IR (dashed line) spectra of standard reaction solutions for carboxylate-based MOFs (zinc nitrate, terephthalic acid, and DEF) at two different water contents: (d) dried solution, (w) water content of $6H_2O$ molecules per zinc ion. The diagram displays the region close to the $\nu_s = 1050$ cm^{-1} frequency of free nitrate. The two vertical lines denote the wavenumbers 1040 and 1027 cm^{-1}, which are attributed to zinc-coordinated nitrate.

In respect to the origin of the O^{2-} ion, it must be stated that there are there two possible sources for it, water and nitrate. An early proposal[37] denotes water as the oxide source (actually OH^-) which, although not explicitly mentioned, can be seen as being generated by reaction 1 followed by the process $OH^-[Zn^{2+}] + HNEt_2 \rightarrow O^{2-}[Zn^{2+}] + (H_2NEt_2)^+$. This view is partly supported by our ^{DEF}pH measurements that reveal a fairly high value for K_a for the first deprotonation step of Zn^{2+}-coordinated water, the polarizing function of the metal ion, and the presence of diethylamine. Formation of hydroxide- and oxide-containing heavy metal terephthalates from hydrates is known at elevated temperatures even in water as a solvent. Examples are $Ni(BDC)\cdot 4H_2O \rightarrow Ni(OH)(HBDC)\cdot H_2O + 2H_2O$ [100 °C, H_2O, 24 h] and $2\ Fe(BDC)\cdot 2H_2O + 1/2O_2 \rightarrow Fe_2O(OH)_2(BDC)\cdot H_2O + 2H_2O + H_2BDC$ [270 °C, H_2O, 1 h].[38] Another argument favoring water as the oxide source is given by the fact that MOF-5 can be generated at low temperatures (25 °C), where most transition-metal nitrate hydrates are stable, simply by diffusing in base from the gas phase.

Alternatively, as we have shown by the water-free experiment, nitrate seems to serve as the sole source for oxide formation as well. Creation of the oxide ion from nitrate seems to be likely in this case because of the strong coordinative destabilization of the nitrate ion by the metal center. Given the fact that almost all solid transition-metal nitrates only exist at room temperature as hydrates and decompose at higher temperatures (but below 100 °C) to metal oxides by giving off crystal water of

crystallization, NO_2, and O_2, the instability of the zinc-coordinated nitrate in a water-free DEF solution at elevated temperatures is plausible.[39] This view is also supported by the observation that from a MOF-5 reaction solution at 100 °C without terephthalic acid precipitation of zinc oxide over the course of several hours occurs accompanied by a color change of the mother solution from colorless to yellow. From the two limiting cases of the MOF-5 formation just discussed, formation in the presence of water at 25 °C and a waterless synthesis at 100 °C, a mixed mechanism model arises for the intermediate temperature and water ranges. Both water and nitrate can serve as the sole source of the oxide ion. Water, however, stabilizes the Zn^{2+}-co-coordinated nitrate ion by reducing the charge transfer from it to the zinc atom, thereby initiating the transition from the nitrate-based oxide formation to a water-based one. On the other hand, the fact that nitrate at high water to zinc ratios (6:) is not fully replaced by water or solvent molecules, as concluded from the vibrational spectroscopy results, may indicate that coordination is still strong enough to destabilize the nitrate ion in such a way that its contribution to oxide formation even in the presence of some water cannot fully be ruled out. In the case of joint coordination the water deprotonation mechanism will certainly dominate. It can be stated, however, that the origin of the oxide ion is unambiguous in both limiting cases, high and no water content.

Since the second deprotonation step in metals that form more stable hydroxides than zinc, like nickel, may not occur under moderate conditions, water-based oxide formation in order to create new oxidic MOF structures may be impossible. In this respect the nitrate decomposition-based solvothermal synthesis we introduced, which requires the absence of water for destabilitzation of the coordinated nitrate ion, may be an option to create these new structures.

Structural Transformations between Zinc Carboxylate Structures. Starting from indications in the literature that MOF-5 is unstable to water exposure, the presumably earliest report of this fact was given by L. Huang,[40] the fundamental question arises under which conditions such transformations occur and how they can be reversed. Since direct transformations of porous MOF structures into one another may open new synthesis routes and yield information about crystal growth properties, we carried out a series of experiments addressing this question. With respect to the water-induced structural transformation it is worth noting some reported facts that demonstrate the important role of water on the structure formation in zinc carboxylates in general. Rosi et al. reliably obtained MOF-69c by adding additional water to the MOF-5 standard recipe.[29] Use of partially hydrolyzed DEF has led to a new structure $Zn_3(NH_2Et_2)_2BDC_4$, which incorporates the solvent hydrolysis product $NH_2Et_2^+$.[41] In a theoretical study Greathouse et al. predicted that the influence of water adsorption in MOF-5 results in its instability for water adsorption exceeding 4 mass %.[42] In order to test this claim qualitatively we exposed MOF-5 still containing the solvent DEF to an approximately water-saturated atmosphere at room temperature (25 °C) while observing structural changes with XRPD. The result can be seen in Figure 6. The existence of a clear XRPD diffractogram demonstrates that a transformation into a new crystal structure occurs instead of an incoherent decay. From the XRPD diffractogram, the resulting structure can be identified as MOF-69c, the hydroxide structure $Zn_3(OH)_2(BDC)_2 \cdot 2DEF$. The figure displays the temporal development of three neighboring diffraction peaks, i.e., for MOF-5 (200), (220) and for MOF-69c (110). The graph demonstrates that within 60 min an almost

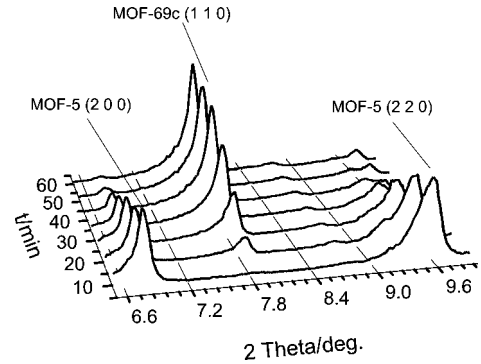

Figure 6. XPRD measurement of the structural transition of DEF-saturated MOF-5 powder into MOF-69c. The powder was kept in a closed cell and exposed to a water-saturated air atmosphere (partial pressure at saturation 3.2 kPa at 25 °C). The transition was completed after 60 min. Crystalline H_2BDC according to the equation $3Zn_4O(BDC)_3 + 8DEF + 5H_2O \rightarrow 4Zn_3(OH)_2(BDC)_2 \cdot 2DEF + H_2BDC$ was not observed.

complete conversion of MOF-5 into MOF-69c has occurred. The theoretical water content contained in the gas-phase filling the pores of the MOF-5 material is with 2.39×10^{-3} wt % at a water partial pressure of 3.17 kPa at 25 °C, much lower than the given instability limit of 4 wt % obtained by Greathouse et al. However, formation of a dense water film at the intrinsic surface by adsorption is quite certain. It is important to note that fully desolvated MOF-5 when exposed to water vapor is much more stable and does not notably decay during the same time period. As a prerequisite, DEF must be present in the MOF-5 structure for conversion into MOF-69c, which is stabilized via hydrogen bonds between the oxygen belonging to the DEF solvent molecule and the SBU (secondary building block) hydroxide. It is noteworthy that rearrangement of the structure is nonstoichiometric with respect to terephthalic acid since MOF-5 containes 3/4 terephthalate units per zinc atom whereas MOF-69c carries only 2/3 units. In order to relate the stability considerations to the standard zinc carboxylate MOF synthesis we exposed the known porous structure MOF-5 as well as MOF-69c and desolvated MOF-69c to various freshly prepared DEF−water mixtures. The amount of material exposed to the solutions (transitions indicated by the full black arrows) was so little that the chemical compositions of the solutions were not significantly altered by the samples added. The results of the exposure after 1 week are shown in Figure 7a. A schematic overview of all structural transformation experiments described in the following is given in Figure 7b. Besides the experiments leading to the Figure 7a, the diagram also lists experiments where reactive environments containing other components than DEF and water were used (dashed arrows) and a thermal treatment experiment (dotted arrow).

Transformation 1: MOF-5 to MOF-69c. MOF-5 was exposed to a mixture of DEF and water at various temperatures (20 °C−100 °C) (Figure 7b dotted arrow). An almost complete transformation within 2 h was observed. The ranges of the water content and temperature values that lead to transformation into MOF-69c can be seen in the phase-diagram-like plot in Figure 7a. Since hydrolysis of DEF is acid catalyzed we assume the DEF−water mixture to be fairly stable. Because of the hydrolysis problem in general, especially at high temperatures, the diagram has to be read as a practical stability diagram for an observation period up to 1 week.

Transformation 2: MOF-69c to MOF69c$_{desolvated}$. MOF-69c is desolvated at 200 °C in an argon stream or under vacuum. The desolvatization occurs in two steps.[28,43] In a thermo-

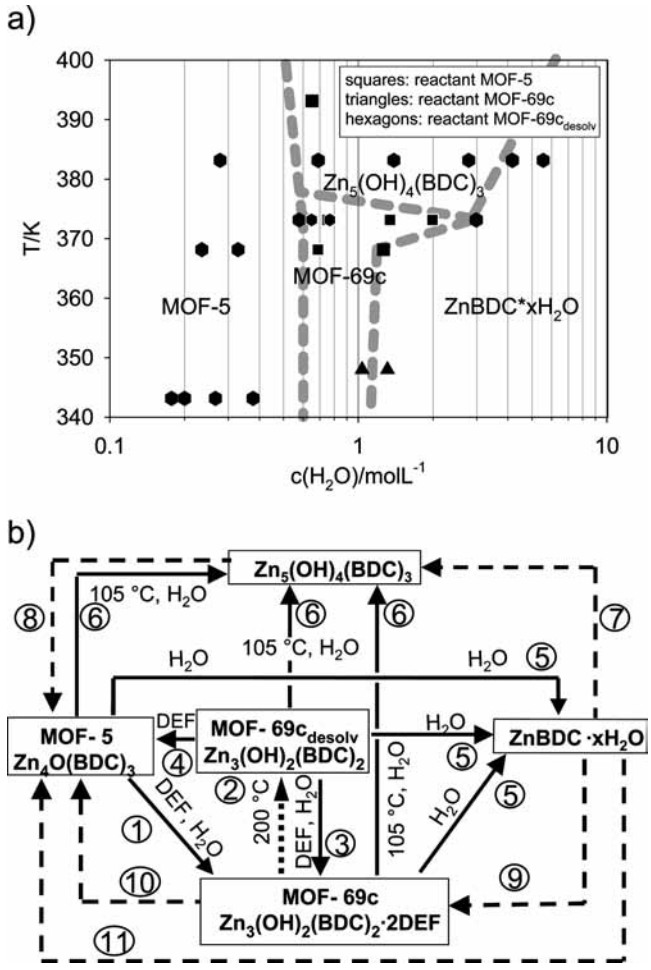

Figure 7. (a) Diagram of the structures resulting from exposure of MOF-5, MOF-69c, and MOF69c$_{desolv}$ to various water−DEF mixtures for a week at the indicated temperatures. (b) Schematic summary of all experiments concerning the thermally and chemically induced structural transformation between various zinc terephthalates (MOFs and simple salts). Only the full arrows correspond to the set of experiments displayed in Figure 7a. The dotted arrow indicates a tempering experiment. The transformations labeled by the dashed arrows denote transformations where components other than DEF and water were used to induce the transition.

gravimetic analysis experiment with a heating rate of 5 K/min we determined the desorption maxima of these steps to be at 210 and 260 °C. The in situ IR analysis of the released gases during this measurement showed only the release of solvent molecules. A possible minor water release would have been below our detection limit.

The fairly strong binding energy of the coordinated two DEF molecules per formula unit demonstrates that they are an essential part of the MOF-69c structures. In the following the term MOF-69c$_{desolvated}$ refers not only to removal of the enclosed solvent molecules but also to the coordinated ones. A XRPD diffractogram taken after desorption of the first DEF molecule from the individual SBUs shows a new phase of an unidentified structure (Figure 8). The same process causes a broad IR band to sharpen to a distinct signal at 3638 cm^{-1}, indicating transition from a μ^3-hydroxide to a singly coordinated one in the resulting structure. Both facts are a clear sign of the destruction of the MOF-69c SBU. Removal of the second solvent molecule per MOF-69c SBU transforms the XRPD diffractogram into a pattern that resembles the original one with respect to the extreme dominance of a single peak, which is a typical feature

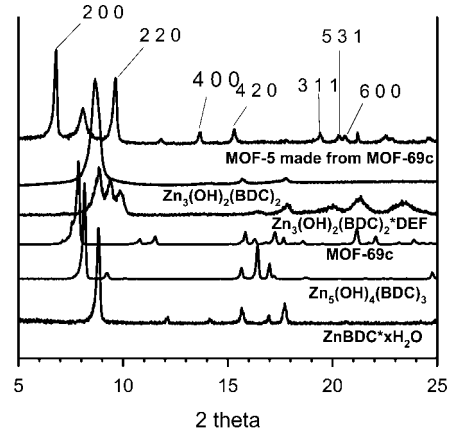

Figure 8. Corresponding XRPD diffractograms of all structures present in the stability diagram in Figure 7. The diffractogram of the intermediate structure $Zn_3(OH)_2(BDC)_2$·DEF produced during the transition from MOF-69c ($Zn_3(OH)_2(BDC)_2$·2DEF) to the fully desolvated structure $Zn_3(OH)_2(BDC)_2$ is also shown.

for layered structures like MOF-69c (Figure 8). Being very broad, this peak also indicates that there is a significant amount of disorder in the structure. The XRPD and IR data demonstrate that the structure is quite different from the starting material.

Transformation 3: MOF-69c$_{desolvated}$ to MOF-69c. Exposure of the singly (one molecule of DEF removed per formula unit) desolvated structure to the solvent DEF with small amounts of water added or exposure of the doubly desolvated structure exposed to large amounts of water at 20 °C will convert the structure back to MOF-69c. Interestingly enough, with dried DEF the transformation was not observed.

Transformation 4: MOF-69c$_{desolvated}$ to MOF-5. Since an attempt to directly transform MOF-69c to MOF-5 simply by exposing it to a DEF−water mixture in which MOF-5 is stable did not succeed, this transformation can be seen as the reverse transition of the MOF-5 to MOF-69c transformation. In contrast to the MOF-69c to MOF-5 transition, MOF-69c$_{desolvated}$ transforms slowly into MOF-5 if exposed to solvent−water mixtures and temperatures in which MOF-5 is stable or to pure DEF (see Figure 7a). From stoichiometric considerations it is clear that there is a lack of terephthalic acid to convert all material into MOF-5 ($3Zn_3(OH)_2(BDC)_2 \rightarrow 2Zn_4O(BDC)_3 + ZnO + 6H_2O$). Consequently, there must remain an excess of ZnO in the material after the transition, which was not visible in the XRPD diffractogram. Hafizovic et al. similarly concluded from their XRPD investigations that some MOF-5 syntheses lead to zinc hydroxide inclusions in the MOF-5 cavities.[44]

Transformation 5: MOF-5, MOF-69c, MOF69c$_{desolvated}$ to ZnBDC·xH$_2$O. This transformation occurs if the indicated structures are exposed to a water−DEF mixture exceeding 0.6 mol/L. The transition in the indicated temperature range happens in less than 24 h for all structures. The XRPD pattern of the ZnBDC·xH$_2$O structure is known from the literature, although the exact crystal structure is not yet solved. Since the XRPD of ZnBDC·xH$_2$O can be observed during the transition from ZnBDC·2H$_2$O to ZnBDC·H$_2$O, x must be between 1 and 2.[45]

Transformation 6: MOF-5, MOF-69c to $Zn_5(OH)_4(BDC)_3$. The transformations occur simply by exposing MOF-5 or MOF-69c to the temperatures and water−solvent mixtures indicated in Figure 7a. Similarly to the previous case, the exact structure of the high-temperature hydroxide $Zn_5(OH)_4(BDC)_3$ is not known but the composition and XRPD pattern can also be found in the literature.[46] The hydroxide content is higher than in MOF-69c. It is noteworthy that the structure $Zn_5(OH)_4BDC_4$ is a high-

temperature phase according to the stability diagram Figure 7a but can also be stabilized at room temperature by the presence of amines.

Transformation 7: ZnBDC·2H$_2$O to Zn$_5$(OH)$_4$(BDC)$_3$. This transformation can be induced by exposing ZnBDC·2H$_2$O to water at pH = 8 at 150 °C and occurs within 48 h.

Transformation 8: Zn$_5$(OH)$_4$(BDC)$_3$ to MOF-5. We did not manage to induce this transition, which formally needs to follow the reaction equation $Zn_5(OH)_4(BDC)_3 \rightarrow Zn_4O(BDC)_3 + ZnO + 2H_2O$. However, to generate MOF-5 this way would be particularly attractive because it may easily allow recovering the solvent DEF in fairly pure form.

Transformation 9: ZnBDC·xH$_2$O (1≤ x≤ 2) to MOF-69c. Just like transformation 8, these transitions do not occur simply by exposing the zinc terephthalate hydrates to DEF or DEF−water mixtures. Nevertheless, ZnBDC·H$_2$O, ZnBDC·2H$_2$O, and the hydrate containing the unknown water content between 1 and 2 can be converted into MOF-69c by exposing them to a 0.1 M Zn(NO$_3$)$_2$·4H$_2$O−DEF solution at 120 °C for 10 h.

Transformation 10: MOF-69c to MOF-5. Direct and complete conversion of MOF-69c into MOF-5 requires stoichiometric addition of terephthalic acid according to

$$4Zn_3(OH)_2(BDC)_2\cdot 2DEF + H_2BDC \rightarrow 3Zn_4O(BDC)_3 + 5H_2O + 8DEF \quad (12)$$

The experiment was carried out by suspending 0.724 mmol of MOF-69c in a solution of 4 mL of DEF with 0.18 mmol of terephthalic acid. After 10 h at 170 °C, MOF-5 was the only phase observable by XRPD.

Transformation 11: ZnBDC·xH$_2$O (1 ≤ x ≤ 2) and ZnBDC·DEF to MOF-5. All known zinc terephthalate hydrates, ZnBDC·H$_2$O, ZnBDC·2H$_2$O, and the hydrate with the unknown water content mentioned in transformation 5, can directly be transformed into MOF-5. For example, ZnBDC·2H$_2$O (1.034 g, 3.9 mmol) exposed to a solution of Zn(NO$_3$)$_2$·4H$_2$O (0.340 g, 1.3 mmol) in DEF (20 mL) is converted to MOF-5 within 10 h at 120 °C.

The zinc terephthalate DEF complex described by Williams et al.[34] that does not contain any water of crystallization can directly be transformed into MOF-5 by suspending it in 0.3 M water-free zinc nitrate DEF solution for 16 h at 140 °C. The preparation of the solution and the reaction was carried out under inert gas conditions to avoid any contamination with water. This experiment needs to be seen as the proof that nitrate in the DEF-based MOF-5 syntheses can serve as the sole source of the oxide ion in MOF-5 according to the reaction

$$3ZnBDC + Zn(NO_3)_2 \rightarrow Zn_4O(BDC)_3 + 2NO_2 + 0.5O_2 \quad (13)$$

Conclusion Structural Transformations. Given the fact that removal of the two DEF molecules from the MOF-69c structure per formula unit required comparably high temperatures as known from the thermogravimetric analysis, it is clear that the energy barrier for the simple conversion of MOF-69c into MOF-5 in a DEF−water mixture in which MOF-5 is stable is too high to be observed in our experiment. The fact that the desolvated structure, if solely exposed to the anhydrous DEF or low water content DEF solution according to Figure 7a, does not react back to MOF-69c but to MOF-5 is surprising since DEF does not possess a strong interaction with the MOF-5 lattice nor is it part of the MOF-5 structure itself. Since DEF can essentially be seen as the original synthesis solution stripped of all highly reactive components, it is less likely that the kinetic aspects of the original synthesis apply. The most natural explanation for the influence of DEF on this transition is that it supports ordering processes by providing a means of material transport. Since the starting material appears to be strongly disordered as seen from the broad XRPD main peak of Zn$_3$(OH)$_2$(BDC)$_2$ (MOF-69c$_{desolvated}$), the ordering process can be seen as a relaxation into the presumably thermodynamically favorable structure at low water conditions. In this respect it is noteworthy that water even accelerates conversion to MOF-5 and increases the total amount of material converted as long as the amount of water does not exceed the limit given in Figure 7a. In the latter case the desolvated structure goes directly back to MOF69c.

From the variety of reactive transformations (i.e., transformations 7−11) we draw the conclusion that the standard synthesis is thermodynamically controlled and that if there are no stoichiometric limitations the thermodynamically most stable structure is formed with quantitative yield. Low water content and temperature of the reaction solution are the most important factors to arrive at MOF-5. If the water content in the standard synthesis is less than 0.6 mol/L MOF-5 is formed. If the temperature is high enough to promote decomposition of zinc-coordinated nitrate, nitrate can serve as the sole source for the oxide ion in MOF-5, as indicated by reaction 13, where no alternative oxygen source like water is available.

4. Summary and Outlook

In the current study we presented a quantitative investigation of the role of the proton activity in the standard MOF-5 synthesis. Most importantly, it was shown that excess Zn(NO$_3$)$_2$·4H$_2$O serves as a buffer to keep the proton activity constant and high enough to prevent rapid deprotonation of the terephthalic acid. This way the second deprotonation step presumably occurs after inclusion into the MOF lattice, thus ensuring a fairly constant precipitation rate and well-ordered crystal growth. There are many ways to make MOF-5, but so far, only the solvothermal method according to Yaghi ensures growth of large well-ordered crystals in a reasonable period of time because of the constant low pH level close to the protolysis equilibrium of the terephthalic acid. The possibility of detecting and controlling the proton activity during the reaction should allow one to control, even electrochemically, the MOF-5 crystal growth properties more precisely. This bears the potential to grow MOF-5 material in forms ranging from nanocrystalline to well-ordered layers if ways can be applied to influence the proton activity without otherwise negatively interfering with the reaction. In addition, if the nonstoichiometric use of zinc nitrate in the standard synthesis is solely required for controlling the proton activity, doing this by other means could help to modify the standard synthesis into a stoichiometric one. As this work demonstrated, stoichiometric syntheses already exist using simple zinc carboxylates as starting materials. These syntheses also allow one to reduce the amount of solvent needed to generate MOF-5, which can significantly reduce production costs if MOF-5 becomes a commercial product. The structural conversions we carried out indicate that formation of MOF-5 or even more generally analogous zinc oxocarboxylates are almost certainly thermodynamically controlled. The investigations concerning the stability of different zinc carboxylate SBUs in various water−DEF mixtures resulted in a phase-diagram-like mapping of the stability regions. In connection to our investigations on the MOF-5 oxide formation, we developed a water-free, nitrate decomposition-based, solvothermal synthesis

variant of Yaghi's standard recipe that may allow one to create new oxidic MOFs that are even more sensitive to water than MOF-5.

Acknowledgment. The authors thank W. Voigt for valuable discussions and Edwin Weber for helping with financial support for S.H.

References and Notes

(1) Eddaoudi, M.; Kim, J.; Rosi, N. L.; Vodak, D. T.; Wachter, J.; O'Keeffe, M.; Yaghi, O. M. *Science* **2002**, *295*, 469.
(2) Chae, H. K.; Siberio-Pérez, D. Y.; Kim, J.; Go, Y.-B.; Eddaoudi, M.; Matzger, A. J.; O'Keeffe, M.; Yaghi, O. M. *Nature* **2004**, *427*, 523.
(3) Rowsell, J. L. C.; Millward, A. R.; Park, K. S.; Yaghi, O. M. *J. Am. Chem. Soc.* **2004**, *126*, 5666.
(4) Wong-Foy, A. G.; Matzger, A. J.; Yaghi, O. M. *J. Am. Chem. Soc.* **2006**, *128*, 3494.
(5) Millward, A. R.; Yaghi, O. M. *J. Am. Chem. Soc.* **2005**, *127*, 17998.
(6) Panella, B.; Hirscher, M. *Adv. Mater.* **2005**, *17*, 538.
(7) Dailly, A.; Vajo, J. J.; Ahn, C. C. *J. Phys. Chem. B* **2006**, *110*, 1099.
(8) Chun, H.; Dybtsev, D. N.; Kim, H.; Kim, K. *Chem. Eur. J.* **2005**, *11*, 3521.
(9) Stallmach, F.; Gröger, S.; Künzel, V.; Kärger, J.; Yaghi, O. M.; Hesse, M.; Müller, U. *Angew. Chem., Int. Ed.* **2006**, *45*, 2123.
(10) Chen, B.; Liang, C.; Yang, J.; Contreras, D. S.; Clancy, Y. L.; Lobkovsky, E. B.; Yaghi, O. M.; Dai, S. *Angew. Chem., Int. Ed.* **2006**, *45*, 1390.
(11) Chen, B.; Yang, Y.; Zapata, F.; Lin, G.; Qian, G.; Lobkovsky, E. B. *Adv. Mater.* **2007**, *19* (13), 1693.
(12) Chen, B.; Yang, Y.; Zapata, F.; Qian, G.; Luo, Y.; Zhang, J.; Lobkovsky, B. *Inorg. Chem.* **2006**, *45* (22), 8882.
(13) Wong, K. L.; Law, G.-L.; Yang, Y.-Y.; Wong, W.-T. *Adv. Mater.* **2006**, *18* (8), 1051.
(14) Sabo, M.; Henschel, A.; Froede, H.; Klemm, E.; Kaskel, S. *J. Mater. Chem.* **2007**, *17* (36), 3827.
(15) Hermes, S.; Schröter, M.-K.; Schmid, R.; Khodeir, L.; Muhler, M.; Tissler, A.; Fischer, R. W.; Fischer, R. A. *Angew. Chem., Int. Ed.* **2005**, *44*, 6237.
(16) Hermes, S.; Schröder, F.; Chelmowski, R.; Wöll, C.; Fischer, R. A. *J. Am. Chem. Soc.* **2005**, *127*, 13744.
(17) Li, H.; Eddaoudi, M.; O'Keeffe, M.; Yaghi, O. M. *Nature* **1999**, *402*, 276.
(18) Yaghi, O. M.; O'Keeffe, M.; Ockwig, N. W.; Chae, H. K.; Eddaoudi, M.; Kim, J. *Nature* **2004**, *423*, 705.
(19) Eddaoudi, M.; Moler, D. B.; Li, H.; Chen, B.; Reineke, T. M.; O'Keeffe, M.; Yaghi, O. M. *Acc. Chem. Res.* **2001**, *34*, 319.
(20) Ferey, G.; Mellot-Draznieks, C.; Serre, C.; Millange, F.; Dutour, J.; Surble, S.; Margiolaki, I. *Science* **2005**, *309*, 2040.
(21) Sabo, M.; Boehlmann, W.; Kaskel, S. *J. Mater. Chem.* **2006**, *16*, 2354.
(22) Arnold, M.; Kortunov, P.; Jones, D. J.; Nedlec, Y.; Kärger, J.; Caro, J. *Eur. J. Inorg. Chem.* **2007**, *60*.
(23) Hermes, S.; Schröder, F.; Chelmowski, R.; Wöll, C.; Fischer, R. A. *J. Am. Chem. Soc.* **2005**, *127*, 13744.
(24) Li, H.; Eddaoudi, M.; O'Keeffe, M.; Yaghi, O. M. *Nature* **1999**, *402*, 276.
(25) Choi, J. Y.; Kim, J.; Jhung, S. H.; Kim, H.-K.; Chang, J.-S.; Chae, H. K. *Bull. Korean Chem. Soc.* **2006**, *27*, 1523.
(26) Hausdorf, S.; Baitalow, F.; Seidel, J.; Mertens, F. O. R. L. *J. Phys. Chem. A* **2007**, *111* (20), 4259.
(27) Liao, J.-H. ; Lee, T.-J.; Su, C.-T. *Inorg. Chem. Commun.* **2006**, *9*, 201.
(28) Loiseau, T.; Muguerra, H.; Ferey, G.; Haouas, M.; Taulelle, F. *J. Solid State Chem.* **2005**, *178* (3), 621.
(29) Kaye, S. S.; Dailly, A.; Yaghi, O. M.; Long, J. R. *J. Am. Chem. Soc.* **2007**, *129* (46), 14176.
(30) Rosi, N. L.; Kim, J.; Eddaoudi, M.; Chen, B.; O'Keeffe, M.; Yaghi, O. M. *J. Am. Chem. Soc.* **2005**, *127*, 1504.
(31) Diggle, J. W.; Parker, A. J. *Aust. J. Chem.* **1974**, *27*, 1617.
(32) Bjerrum, N. *Z. Phys. Chem.* **1905**, *63*, 428.
(33) Kaduk, J. A. *Acta Crystallogr., Sect. B* **2000**, *56*, 474.
(34) Williams, C. A. *Chem. Commun.* **2005**, 5435.
(35) Sze, Y.-K.; Irish, D. E. *J. Sol. Chem.* **1978**, *7* (6), 395.
(36) Sze, Y.-K.; Irish, D. E. *J. Sol. Chem.* **1979**, *8* (5), 395.
(37) Rosi, N. L.; Eckert, J.; Eddaoudi, M.; Vodak, D. T.; Kim, J.; O'Keefe, M.; Yaghi, O. M. *Science* **2003**, *300*, 1127.
(38) Sherif; Fawzy, G. *Ind. Eng. Chem. Prod. Res. Dev.* **1970**, *9* (3), 408.
(39) Ewing, W. W.; Brandner, J. D.; Guyer, W. R. F. *J. Am. Chem. Soc.* **1939**, *61*, 260.
(40) Huang, L.; Wang, H.; Chen, J.; Wang, Z.; Sun, J.; Zhao, D.; Yan, Y. *Microporous Mesoporous Mater.* **2003**, *58* (2), 105–114.
(41) Burrows, A. D.; Cassar, K.; Friend, R. M.W.; Mahon, M. F.; Rigby, S. P.; Warren, J. E. *CrystEngComm* **2005**, *7*, 548.
(42) Greathouse, J. A.; Allendorf, M. D. *J. Am. Chem. Soc.* **2006**, *128* (33), 10678.
(43) Liao, J. H.; Huang, W. C. *Inorg. Chem. Commun.* **2006**, *9*, 201.
(44) Hafizovic, J.; Bjorgen, M.; Olsbye, U.; Dietzel, P. D. C.; Bordiga, S.; Prestipino, C.; Lamberti, C.; Lillerud, K. P. *J. Am. Chem. Soc.* **2007**, *129* (12), 3612.
(45) Thirumurugan, A.; Rao, C. N. R. *J. Mater. Chem.* **2005**, *15*, 3852.
(46) Carton, A.; Abdelouhab, S.; Renaudin, G.; Rabu, P.; Francois, M. *Solid State Sci.* **2006**, *8*, 958.

JP7110633